SUPPLEMENTARY APPENDIX

Ddx41 inhibition of DNA damage signaling permits erythroid progenitor expansion in zebrafish

Joshua T. Weinreb,[1,2] Varun Gupta,[3] Elianna Sharvit,[1] Rachel Weil,[1] and Teresa V. Bowman[1,2,4]

[1]Albert Einstein College of Medicine, Department of Developmental and Molecular Biology; [2]Albert Einstein College of Medicine, Gottesman Institute for Stem Cell Biology and Regenerative Medicine; [3]Albert Einstein College of Medicine, Department of Cell Biology and [4]Albert Einstein College of Medicine and Montefiore Medical Center, Department of Medicine (Oncology), Bronx, NY, USA

 doi:10.3324/haematol.2020.257246

Received: April 28, 2020.

Accepted: March 16, 2021.

Pre-published: March 25, 2021.

Correspondence: *TERESA V. BOWMAN* - teresa.bowman@einsteinmed.org

Ddx41 inhibition of DNA damage signaling permits erythroid progenitor expansion in zebrafish

Joshua T. Weinreb[1,2], Varun Gupta[3], Elianna Sharvit[1], Rachel Weil[1], Teresa V. Bowman[#1,2,4]

1. Albert Einstein College of Medicine, Department of Developmental and Molecular Biology, Bronx, NY, USA
2. Albert Einstein College of Medicine, Gottesman Institute for Stem Cell Biology and Regenerative Medicine, Bronx, NY, USA
3. Albert Einstein College of Medicine, Department of Cell Biology, Bronx, NY, USA
4. Albert Einstein College of Medicine and Montefiore Medical Center, Department of Medicine (Oncology), Bronx, NY, USA

SUPPLEMENTARY FIGURE

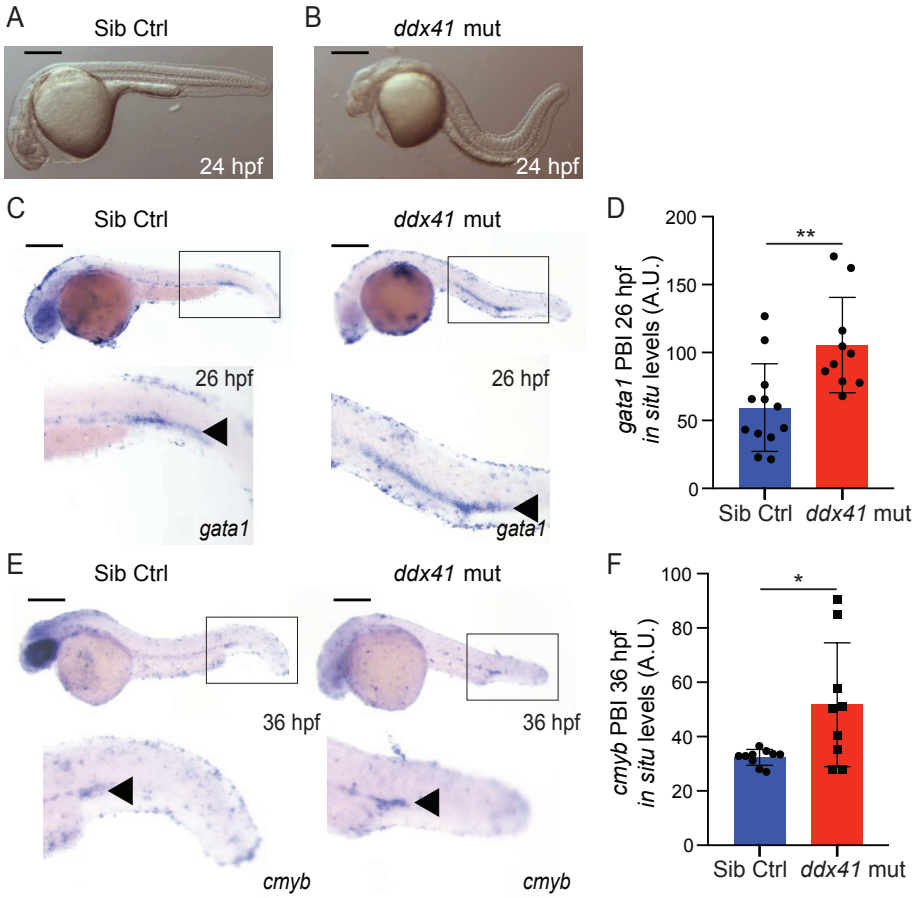

Supplemental Figure S1. Ddx41 regulates erythroid-myeloid progenitor levels *in vivo*.
A,B. Brightfield images of sibling controls (A) and *ddx41* mutants (B) at 24 hpf showing morphological differences, such as body curvature and mild brain death. Scale bars=250μm. **C,E**. *In situ hybridization* of *gata1* at 26 hpf (C) [Scale bars=250μm] and *cmyb* at 36 hpf (E) [Scale bars=350μm] in sibling controls (left) and *ddx41* mutants (right). **D,F**. Quantification of PBI *gata1* (D) and *cmyb* (F) *in situ hybridization* levels from (C) and (E), respectively. Quantification was done using Fiji. Graphs display means ± standard deviations (stds) with p-values calculated with unpaired Student's t-test, *p<0.05, **p≤0.01. For in situ hybridization, n≥10 embryos per experiment.

SUPPLEMENTARY TABLE LEGENDS

Table S1. Differential gene expression.

DE-Seq2 differentially expressed genes in *gata1:dsred*+ erythrocytes in ddx41 mutants vs. siblings

Table S2. Pathway analysis on downregulated genes.

Reactome Pathways - downregulated genes in *ddx41* mutant vs. sibling *gata1:dsred*+ erythrocytes

Table S3. Pathway analysis on upregulated genes.

Reactome Pathways - upregulated genes in *ddx41* mutant vs. sibling *gata1:dsred*+ erythrocytes

Table S4. Differentially spliced genes.

Splicing analysis in sibling vs. *ddx41* mutant *gata1:dsred*+ erythrocytes

Table S5. Changes to protein sequence from alternative splicing.

Prediction of splicing outcome on protein coding regions

Table S6. Pathway analysis of alternatively spliced genes.

Pathways enriched in alternatively spliced factors with NMD vs. protein sequence changes (non-NMD)

Table S7. Primer sequences.

Primers used in this study for genotyping and RT-qPCR.

METHODS

EXPERIMENTAL MODEL AND SUBJECT DETAILS

Zebrafish

Zebrafish were maintained as described (1). All fish were maintained according to IACUC-approved protocols in accordance with Albert Einstein College of Medicine research guidelines. We utilized several established zebrafish lines. Genotyping and phenotyping to confirm their identity was performed for each new generation and for embryos. Mutants for *ddx41* (*ddx41*^{sa14887}) were acquired from the Zebrafish International Resource Center as part of the Sanger Institute Zebrafish Mutation Project (2). The mutation results in a premature stop codon at Tyrosine 410. There is maternally-derived Ddx41 protein as detected by immunofluorescence that decreases in the mutants as the animals develop, suggesting the mutants are zygotic nulls. As early as 24 hpf, there appears to be slight brain death and abnormal curvature of the tail in *ddx41* homozygous mutants, allowing for phenotypic identification of mutants compared to siblings based on morphology (Figure S1A-B). Homozygous mutants are embryonic lethal dying by 3 dpf due to the depletion of maternal Ddx41 stores. This suggests that *ddx41* mutants should be considered functional hypomorphs. This allows for the assessment of primitive and definitive hematopoietic development in zebrafish up to 3 dpf, but precludes the assessment of hematopoiesis beyond this point. For all experiments, *ddx41* homozygous mutants are compared to

sibling controls, which are a mix of heterozygotes and wild types. In addition to *ddx41* mutants, *gata1*:dsred (3) transgenics were used and scored for dsRED fluorescence within erythrocytes. The genotyping for *ddx41* was determined by mutant-specific PCR, which was initially verified by Sanger sequencing. Additionally, the genotype of *ddx41*$^{sa14887/+}$ carriers were validated by paired mating of heterozygous adult animals followed by examination of embryos for the expected homozygous recessive phenotype. Genomic DNA for genotyping was isolated by alkaline lysis (4). The *ddx41*^{sa14887} mutant and wild-type-specific PCR products were analyzed by gel electrophoresis. Genotyping primers are provided in Table S7.

Drug treatments

All drugs were dissolved in DMSO. Dilutions were made in E3 embryo water. Concentrations used for experiments were 30nM for KU60019 (ATM inhibitor; Fisher Scientific) and 30nM for AZ20 (ATR inhibitor; Fisher Scientific). DMSO in E3 embryo water was used as the vehicle control.

Whole-mount *in situ* hybridization and o-dianisidine staining

In situ hybridization steps were performed as described previously by Thisse *et al.* (5) with minor modifications: before proteinase K permeabilization, embryos older than 28 hpf were bleached after re-hydration to remove pigmentation. The bleaching was done for 5-10 minutes using a bleaching solution of 0.8% KOH, 0.9% H_2O_2 and 0.1% Tween 20. Embryos were then scored manually, imaged and genotyped. The *βe3-globin* (6), *cmyb (7)*, and *gata1 (8)* probes were used, and *in situ* levels were quantified using FIJI in a similar manner to previously described methods (9).

O-dianisidine staining was performed as described previously (10). Briefly, dechorionated live embryos were soaked in o-dianisidine staining solution (0.62 mg/mL o-dianisidine [Sigma-Aldrich], 10.9 µM sodium acetate, and 0.65% H_2O_2) for 10 minutes in the dark, then rinsed in phosphate-buffered solution plus 0.1% Tween 20 (PBT) twice and observed under the microscope. Afterward, embryos were preserved in a 4% paraformaldehyde (PFA) solution.

Flow cytometry

At 28 or 40 hpf, mutant and sibling embryos were binned based on morphological differences. For generation of single-cell suspensions, 10-20 embryos were first removed from their chorions using pronase (Roche), and then homogenized by manual dissociation using a sterile razor blade followed by digestion with Liberase (Roche). For the digestion, dissociated embryos were resuspended in 600 µl 1× Dulbeccos-PBS (D-PBS) (Life Technologies) supplemented with a 1:65 dilution (9.23 µl) of 5

mg/ml Liberase and then incubated at 37°C for 7 minutes. The reaction was stopped with the addition of 5% (30 μl) fetal bovine serum (FBS) (Life Technologies). The cells were then filtered through a 40-μm cell strainer (Falcon) and pelleted by centrifugation at 3000 rpm for 5 minutes. Cell pellets were resuspended in 400-700 μl FACS buffer (0.9× D-PBS, 5% FBS, 1% Penn/Strep (Life Technologies)). DAPI (4′,6-diamidino-2-phenylindole) was added to a final concentration of 1 μg/ml to facilitate exclusion of dead cells from the analysis. Samples were analyzed with a LSRII flow cytometer (BD Biosciences) and FlowJo software. Cells from non-fluorescent embryos were used to set gates above background. Quantification for the absolute number of cells was performed by acquiring all events in a tube on the flow cytometer to determine the total number of target cells. This number was then divided by the total number of embryos analyzed to calculate the number of target cells per embryo.

Cell cycle and apoptosis analysis

For 5-ethynyl-2′-deoxyuridine (EdU) incorporation experiments, 28 hpf embryos were binned into 6 well plates, with ~30 embryos per well. Embryos were incubated with 20 mM EdU for 2 hours. Generation of single-cell suspensions of 40 hpf embryos was accomplished as described above. EdU was detected using the Click-IT EdU Flow Cytometry Assay Kit according to the manufacturer's instructions (Invitrogen C10424). Flow cytometry analysis for active caspase-3 at 30 hpf was performed as previously described (11). Samples were analyzed with a LSRII flow cytometer (BD Biosciences) and FlowJo software.

RNA-sequencing and splicing analysis

Erythrocytic progenitors from *ddx41* mutants and siblings at 40 hpf were isolated by fluorescently-activated cell sorting (FACS) on a Mo-Flo cell sorter (Beckman Coulter). RNA from these cells was subsequently isolated using the Zymo Quick-RNA microprep kit (R2080) according to the manufacturer specification. The TURBO DNA-free kit (Life Technologies) was used for DNA removal following RNA extraction. RNA and library quality was assessed using a bioanalyzer Pico Chip (Agilent) by the Einstein Genomics core facility. Libraries for RNA samples with RIN≥9 were prepared by BGI using the Nugene low-input RNA sequencing kit. Five independent biological replicates were analyzed. On average, approximately 30 million paired-end 150 base pair sequencing reads were acquired per sample using the Illumina NovoSeq platform. All data are deposited under GEO accession number GSE160979. DE-Seq2 (12) was used to determine differential gene expression (defined as log2 fold change $\geq |1|$, FDR $p<0.05$) between *ddx41* mutant and sibling control erythrocytes. Differential inclusion rates of splicing events between *ddx41* mutants and siblings were calculated using rMATS (13) (replicate Multivariate Analysis of Transcript Splicing, version 4.0.2). Splicing events with inclusion differences ≥ 10% and

FDR ≤ 0.01 were considered significantly altered. After obtaining alternatively spliced events from rMATS, we calculated whether any of these spliced events would lead to protein sequence alterations or promote nonsense-mediated decay (NMD) of the splice variant. First, a refFlat file was downloaded from UCSC (for appropriate zebrafish version 10). It contains the information of the coding frames for all the annotated exons. Custom-based PERL scripts were used along with refFlat and rMATS output files for skipped exon (SE) and retained intron (RI) spliced events to obtain sequences for both the wild-type and alternative splice variant transcripts. These sequences were then converted to protein sequences with stop codon positions and altered protein sequences calculated for all variants. Pathway analysis was analyzed using the Molecular Signatures Database (MSigDB) or PANTHER (14-17).

RT-qPCR

To validate the RNA-sequencing data, we performed reverse transcription (RT) quantitative PCR. RNA was isolated from 40 hpf embryos using TRIzol (ThermoFisher) followed by DNA removal with TurboDNase (ThermoFisher). High-capacity cDNA synthesis kit (ThermoFisher) was used to generate cDNA. Real-time quantitative PCR was performed with PowerSYBR (ThermoFisher) on a QuantStudio 5 384-well instrument (ThermoFisher). Analysis was performed with Design Analysis 2 software with fold-change calculated via the $\Delta\Delta$Ct method. Primer sequences are listed in Table S7. For quantification of embryonic and larval globins, values were normalized to the erythrocyte-specific gene *slc4a1,* which encodes Band3, as previously described (18). For quantifying cell cycle-related genes, values were normalized to β-actin.

Single-cell immunofluorescence of zebrafish embryonic cells

Single-cell suspensions were prepared as described above, and cell staining was performed as described in Sorrells & Nik *et al.* (19). The rabbit polyclonal anti-zebrafish γH2AX primary antibody (GeneTex GTX127342) was used at a dilution of 1:500. All antibodies were diluted in blocking buffer (5% bovine serum albumin (BSA)/0.2% milk/PBS) and incubated for 3 h at room temperature followed by 3 washes in PBT. The goat anti-rabbit AlexaFluor-594 (Thermo Fisher Scientific) was used at a dilution 1:1000 and incubated for 1 h at room temperature followed by 3 washes in PBT. After final washes, cells were mounted with DAPI-Fluoromount-G (Southern Biotech), covered with a 25×25 mm glass coverslip and sealed with clear nail polish. Fluorescence intensity measurements of γH2AX were performed using FIJI.

May-Grunwald Giemsa staining of primitive erythroid cells

This protocol was performed as described by (20). Erythrocytes were isolated via two methods. At 40 hpf, *gata1:dsred*$^{+}$ cells were isolated by FACS. Alternatively, two-day old embryos were placed on poly-L-lysine coated slides in a drop of 1× D-PBS + 1% bovine serum albumin (Sigma). Blood cells were released from the embryo by puncturing the pericardial sac and upper yolk sac with fine forceps. The slides were air-dried at room temperature prior to staining. For staining, slides were immersed in undiluted May-Grunwald stain (Eng Scientific May-Grunwald stain solution 1, Fisher Scientific) for 2 minutes and briefly rinsed in ddH_20. Slides were then immersed in diluted Giemsa stain (diluted 1:4 with milliQ water) for 20 minutes (Eng Scientific May-Grunwald stain solution II, Fisher Scientific) and briefly rinsed in ddH_20. Once slides were dry, a drop of Permount solution (Fisher Scientific) was added and slides were covered with a 25×25 mm glass cover slip and left overnight to dry. Once slides were dry, the cells were visualized with a 63× oil-immersion lens.

Image acquisition and processing

Brightfield and fluorescent images were acquired using a Zeiss Axio Discovery.V8 with an AxioCam HRc camera. Confocal images for zebrafish single-cell immunofluorescence were acquired using a Leica SP5 AOBS Inverted DMI6000 microscope with a 63X oil objective and zoomed in fields were taken at 6.5X zoom. FIJI/ImageJ was used for quantification of images (21). Flowjo, GraphPad Prism 8, Adobe Photoshop and Adobe Illustrator were used to generate figures.

Statistics

Experiments were performed with a minimum of three replicates. Statistical analyses were performed as indicated in each figure using unpaired Student's t-test or a one-way ANOVA with Tukey's multiple testing correction as appropriate; error bars indicate the standard deviation of mean, unless otherwise indicated.

REFERENCES

1. Lawrence C. Advances in zebrafish husbandry and management. Methods Cell Biol. 2011;104:429-451.

2. Kettleborough RN, Busch-Nentwich EM, Harvey SA, et al. A systematic genome-wide analysis of zebrafish protein-coding gene function. Nature. 2013;496(7446):494-497.

3. Traver D, Paw BH, Poss KD, et al. Transplantation and in vivo imaging of multilineage engraftment in zebrafish bloodless mutants. Nat Immunol. 2003;4(12):1238-1246.

4. Meeker ND, Hutchinson SA, Ho L, Trede NS. Method for isolation of PCR-ready genomic DNA from zebrafish tissues. Biotechniques. 2007;43(5):610, 612, 614.

5. Thisse C, Thisse B. High-resolution in situ hybridization to whole-mount zebrafish embryos. Nat Protoc. 2008;3(1):59-69.

6. Brownlie A, Hersey C, Oates AC, et al. Characterization of embryonic globin genes of the zebrafish. Dev Biol. 2003;255(1):48-61.

7. Liao EC, Paw BH, Oates AC, et al. SCL/Tal-1 transcription factor acts downstream of cloche to specify hematopoietic and vascular progenitors in zebrafish. Genes Dev. 1998;12(5):621-626.

8. Detrich HW, 3rd, Kieran MW, Chan FY, et al. Intraembryonic hematopoietic cell migration during vertebrate development. Proc Natl Acad Sci U S A. 1995;92(23):10713-10717.

9. Dobrzycki T, Krecsmarik M, Bonkhofer F, Patient R, Monteiro R. An optimised pipeline for parallel image-based quantification of gene expression and genotyping after in situ hybridisation. Biol Open. 2018;7(4).

10. Lieschke GJ, Oates AC, Crowhurst MO, Ward AC, Layton JE. Morphologic and functional characterization of granulocytes and macrophages in embryonic and adult zebrafish. Blood. 2001;98(10):3087-3096.

11. Sorrells S, Nik S, Casey M, et al. Spliceosomal components protect embryonic neurons from R-loop-mediated DNA damage and apoptosis. Dis Model Mech. 2018;11(2).

12. Love MI, Huber W, Anders S. Moderated estimation of fold change and dispersion for RNA-seq data with DESeq2. Genome Biol. 2014;15(12):550.

13. Shen S, Park JW, Lu ZX, et al. rMATS: robust and flexible detection of differential alternative splicing from replicate RNA-Seq data. Proc Natl Acad Sci U S A. 2014;111(51):5593-5601.

14. Subramanian A, Tamayo P, Mootha VK, et al. Gene set enrichment analysis: a knowledge-based approach for interpreting genome-wide expression profiles. Proc Natl Acad Sci U S A. 2005;102(43):15545-15550.

15. Liberzon A, Birger C, Thorvaldsdottir H, et al. The Molecular Signatures Database (MSigDB) hallmark gene set collection. Cell Syst. 2015;1(6):417-425.

16. Mi H, Muruganujan A, Thomas PD. PANTHER in 2013: modeling the evolution of gene function, and other gene attributes, in the context of phylogenetic trees. Nucleic Acids Res. 2013;41(Database issue):D377-86.

17. Thomas PD, Campbell MJ, Kejariwal A, et al. PANTHER: a library of protein families and subfamilies indexed by function. Genome Res. 2003;13(9):2129-2141.

18. Ganis JJ, Hsia N, Trompouki E, et al. Zebrafish globin switching occurs in two developmental stages and is controlled by the LCR. Dev Biol. 2012;366(2):185-194.

19. Sorrells S, Nik S, Casey M, et al. Spliceosomal components protect embryonic neurons from R-loop-mediated DNA damage and apoptosis. Dis Model Mech. 2018.

20. De La Garza A, Cameron RC, Nik S, Payne SG, Bowman TV. Spliceosomal component Sf3b1 is essential for hematopoietic differentiation in zebrafish. Exp Hematol. 2016;44(9):826-837.

21. Collins TJ. ImageJ for microscopy. Biotechniques. 2007;43(1 Suppl):25-30.